

Analysis of Pavement Deterioration Using three-dimensional Finite Elements Technique

Ahmed Mohamady, Abu-Bakr M. Elhady, and Mohamed S. Eisa

¹ Assoc. Prof. of Highways and Airports Engineering, Faculty of Engineering, Zagazig University, Egypt

² Egyptian Space Program

³ PhD candidate, Faculty of Engineering, Zagazig University, Egypt

Abstract: - Three-dimensional Finite elements models have been used to describe stress and strain response parameters for steel wire grid reinforced flexible pavement sections. In this study three paving sections were analyzed. The first section represents one of the commonly sections used in the paving of local roads, the second section is commonly used in expressways and the third section is used in freeways. Study was conducted using Finite element computer package ADINA. The reinforcement was arranged at different depths. Steel wire grid reinforced sections results are compared to geosynthetics grid reinforced sections as well as typical rigid pavement section commonly used in Egypt. The analysis showed that the best location of reinforcement is at bottom of base layer. Comparisons show that steel mesh reinforced sections characteristics improved than geosynthetics grids reinforced sections and are almost close to rigid section.

Keywords: - 3-D finite elements, paving sections, geosynthetics grids, rigid pavement, steel wire grid

I. INTRODUCTION

Increasing truck loads on Egyptian road network Also several locations of low speeds were introduced due to high traffic volumes. All of these may cause several pavement distresses. The most common distress types occurring in the Egyptian roads are rutting and cracking, sags, corrugations, etc. Pavement distresses cause many troubles to the vehicles and users [1,2]. The maintenance of such distresses may need high budget and time consuming and hence cause traffic trouble during maintenance and repair processes. The design of flexible pavements is largely based on empirical methods. However, there is currently a shift underway towards more mechanistic design techniques. Finite element (FE) methods have generally been used to determine stresses, strains and displacements in flexible pavement [3-5].

II. OBJECTIVES AND METHODOLOGY

This paper investigate the paving sections used in places that have vehicles to reduce speed as a result of traffic and the presence of some speed sedatives like railway crossing and town entrances also at places of U-turns to opposite directions. This study also aims to strengthen the pavement layers of these sections with steel wire grid or geosynthetics grids at different depths and effect of this strengthen to reduce the stresses on the pavement sections and hence increasing the pavement life. Three paving sections were studied; local road section, expressway section and freeway section. The proposed layers thicknesses and the associated properties for the investigated sections are shown in Tables (1) to (3) [10,11]. These sections rested on infinite subgrade soil and its modulus of elasticity is 50 MPa and value of poisson's ratio is 0.25. The reinforcement materials are steel wire grid or geosynthetics grids with wire diameter 4mm and square cell side length 10cm and its properties were given in Table (4)[6,7]. In local road section, the locations of strengthening were chosen at bottom of wearing surface, middle of base and bottom of base, while in expressway section the locations of strengthening were chosen at bottom of wearing surface, bottom of binder layer, middle of base and bottom of base, finally the locations of strengthening in freeway section were chosen at bottom of wearing surface, bottom of binder layer, bottom of bituminous base, middle of base and bottom of base. The reinforced sections were

compared with typical rigid pavement section commonly used in Egypt to evaluate the proposed strengthening technique.

III. FINITE ELEMENTS MODELING (FEM)

Considering the studied sections are modeled as multilayer semi finite elements. All materials are treated as homogeneous and isotropic. Deformations are considered very small relative to the dimensions so the equation of liner elasticity is valid [12].

3.1 ADINA computer program

The multi-purpose finite element program ADINA version 8.7 [9] was used to model 3-D finite element analysis. All materials was modeled as 3D-solid elements as 8- node. This type of node gives a high level of accuracy in combination with an acceptable computing time demand.

3.2 Boundary conditions and loading

The boundary conditions and loading of static analysis for selected sections are shown in Fig (1). It can be observed that the bottom of the pavement is fixed at X, Y and Z translations while the sides of pavement are restricted with Z translation only.

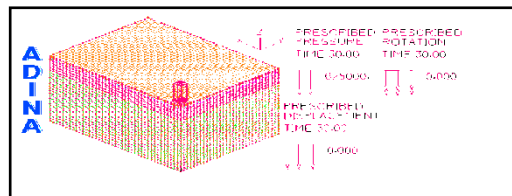


Fig.1. FEM model for freeway section

IV. NUMERICAL RESULTS

In pavement design the most important parameter is the stress distribution as vertical compressive stress and lateral tensile strain shown in fig (2).The investigated cases were modeled with ADINA program and the results were presented and discussed here in after.

4.1 Results of sections affected by vertical loads

4.1.1 Vertical stress

The variation of vertical stress σ_z at bottom of base layer in studied sections due to vertical pressure of wheel is presented in figures (3) to (8). Figures illustrate the effect of adding reinforcement with different locations. Figures (3) and(4)for local road section display that the vertical stress σ_z in without reinforcement case decrease gradually from $-5.54E+04$ Pa under the middle of the wheel load to vanished at the surface, and shows that there is no change in cases reinforcement at bottom of wearing surface. Figures also show that there is a noticeable change when steel reinforcement was arranged at middle of base layer , the vertical stress σ_z under the center line of the wheel load decreased to $-5.32+04$ Pa i.e.19% from without reinforcement case, while for case of reinforcement with geosynthetic there is no change. Figures illustrate that there is a drastic change in vertical stress σ_z values when the steel reinforcement was added at bottom of base layer, the vertical stress σ_z under the center line of the wheel load decreased to $-2.89+04$ Pa i.e.48% from without reinforcement case, while in case of reinforcement with geosynthetic arrived to $-3.57+04$ Pa i.e.35.6% from without reinforcement case.

Table 1. Layers thickness and the associated properties for local road section

Layer	Modulus of elasticity (MPa)	Possion's ratio	Density (KN/m ³)	Thickness (mm)
Wearing surface	2757.91	0.30	22	50
Base	275.791	0.20	20	300
Subgrade	50	0.25	17	Infinite

Table 2. Layers thickness and the associated properties for expressway section

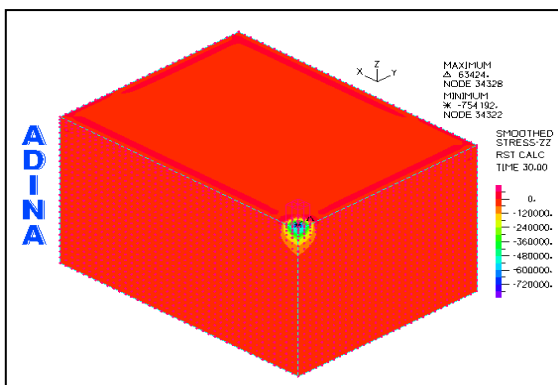
Layer	Modulus of elasticity (MPa)	Possion's ratio	Density (KN/m ³)	Thickness (mm)
Wearing surface	2757.91	0.30	22	50
Binder	2757.91	0.30	22	50
Base	275.791	0.20	20	400
Subgrade	50	0.25	17	Infinite

Table 3. Layers thickness and the associated properties for freeway section

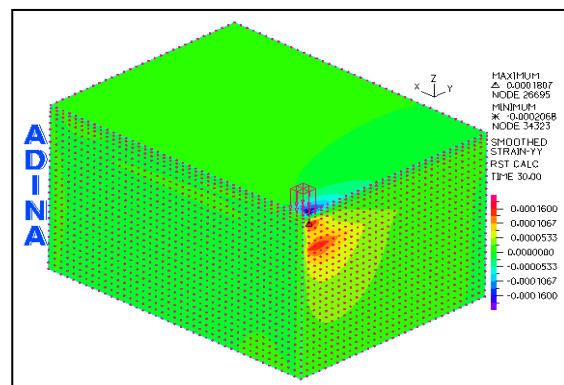
Layer	Modulus of elasticity (MPa)	Possion's ratio	Density (KN/m ³)	Thickness (mm)
Wearing surface	2757.91	0.30	22	50
Binder	2757.91	0.30	22	50
Bit. base	2413.16	0.35	21	70
Base	275.791	0.20	20	400
Subgrade	50	0.25	17	Infinite

Table 4. Properties of reinforcing materials

Material	Modulus of elasticity (MPa)	Possion's ratio	Density (KN/m ³)
Steel	210000	0.25	78.50
Geosynthetics	4230	0.35	18.00



(a)



(b)

Fig.2. (a) Vertical stress σ_z (b) Lateral strain ϵ_y

Figures (5) and (6) for expressway section illustrate that the vertical stress σ_z in without reinforcement case start decrease from $-3.94E+04Pa$ under the middle of the wheel load to decay at the surface, and show that there is no change in cases reinforcement at bottom of wearing surface, at bottom of binder layer. Figures also show that there is a noticeable change when the steel reinforcement was arranged at middle of base layer, in this location the vertical stress σ_z under the center line of the wheel load decreased to $-3.74+04 Pa$ i.e.18% from without reinforcement case, while for case of reinforcement with geosynthetic there is no change. Figures also illustrate that there is a drastic change in vertical stress σ_z values when the steel reinforcement was added at bottom of base layer. The vertical stress σ_z under the center line of the wheel load decreased to $-2.05+04 Pa$ i.e.48% from without reinforcement case. In case of reinforcement with geosynthetic arrived to $-2.55+04Pa$ i.e.35.50% from without reinforcement case.

Figures (7) and (8) for freeway section show the vertical stress σ_z in without reinforcement case start decrease from $-3.27E+04Pa$ under the middle of the wheel load to zero Pa at the surface. Figures show that there is no change in cases reinforcement at bottom of wearing surface, bottom of binder layer and bottom of bituminous base layer. Figures also show that there is a noticeable change when we add the steel reinforcement at middle of base layer, in this location vertical stress σ_z under the center line of the wheel load decreased to $-3.00+04 Pa$ i.e. 8% from without reinforcement case while for case of reinforcement with geosynthetic there is no change. Figures illustrate that there is a drastic change in vertical stress σ_z values when the reinforcement was at bottom of base layer, vertical stress σ_z under the center line of the wheel load decreased to $-1.70+04 Pa$ i.e.48% from without reinforcement case, while in case of reinforcement with geosynthetic arrived to $-2.13+04Pa$ i.e.35% from without reinforcement case.

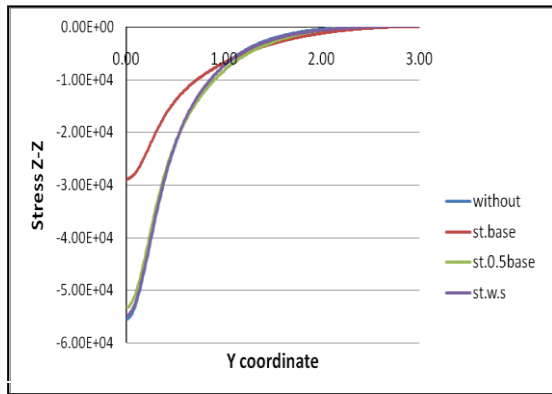


Fig. 3. Vertical stress σ_z due to vertical pressure of wheel at bottom of base layer for local road section with and without steel reinforcement

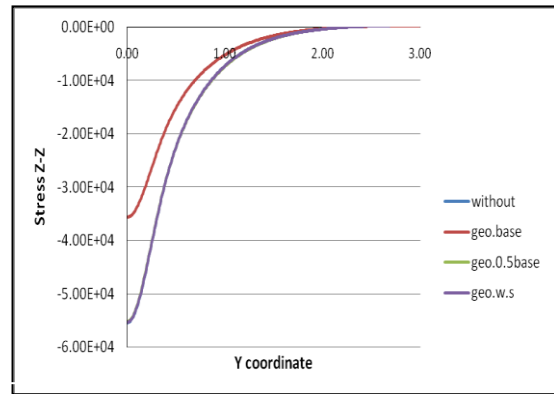


Fig. 4. Vertical stress σ_z due to vertical pressure of wheel at bottom of base layer for local road section with and without geosynthetics reinforcement

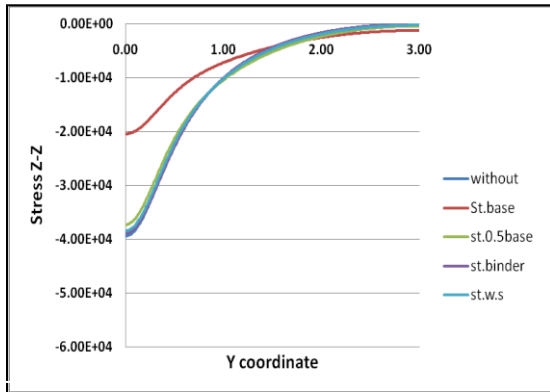


Fig. 5. Vertical stress σ_z due to vertical pressure of wheel at bottom of base layer for expressway section with and without steel reinforcement

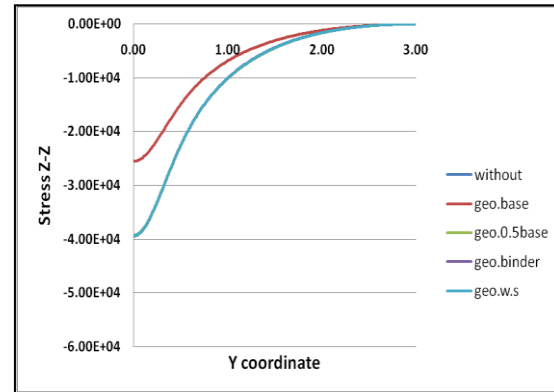


Fig. 6. Vertical stress σ_z due to vertical pressure of wheel at bottom of base layer for expressway section with and without geosynthetics reinforcement

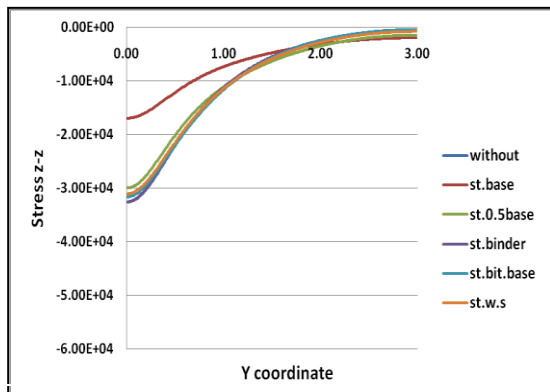


Fig. 7. Vertical stress σ_z due to vertical pressure of wheel at bottom of base layer for freeway section with and without steel reinforcement

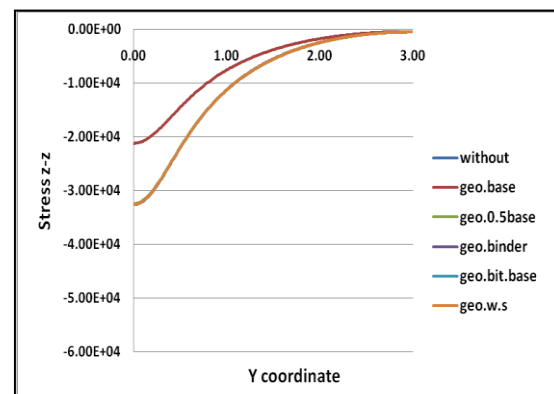


Fig. 8. Vertical stress σ_z due to vertical pressure of wheel at bottom of base layer for freeway section with and without geosynthetics reinforcement

4.1.2 Lateral strain

For studied sections the lateral strain ϵ_y variation versus section depth under center of wheel pressure are presented in figures (9) to (14). Figures present comparison of lateral strain variation in sections without and with reinforcement at different depths. It is depicted that for the case without reinforcement the lateral strain starts with negative value at top of wearing surface layer and rapidly increases to zero approximately at middle of wearing surface layer then continue increases to the maximum value at bottom of base layer and vanished at

the end of section. The maximum lateral strain ϵ_Y values at bottom of base layers in sections A, B and C are $4.91E-04$, $3.59E-04$ and $2.92E-04$ respectively. For reinforced section the lateral strain behavior the same as unreinforced sections but it is confined at the reinforcement location.

Figures (9) and (10) for local road section show when we add the steel reinforcement at the middle of base layer the lateral strain ϵ_Y is decreased to $4.44E-05$ i.e. decreasing percent is 80.35% from without reinforcement case ($1.92E-04$) then arrived to $3.73E-04$ at bottom of base layer i.e. 24.12% decreasing percent from the strain in original case. Figures also illustrate that there is a drastic change the lateral strain ϵ_Y values when the steel reinforcement at bottom of base layer, lateral strain ϵ_Y in this location was $6.52E-05$ i.e. decreasing percent is 86.70% from its value in without reinforcement case. While in case of reinforcement with geosynthetic at same location the lateral strain ϵ_Y was $4.12E-04$ i.e. decreasing percent is 16.00% from its value in without reinforcement case. Also show there are no change in lateral strain ϵ_Y distribution for others cases and case without reinforcement.

Figures (11) and (12) for expressway section show that there is no change in the strain values in cases of steel or geosynthetic reinforcement at bottom of wearing surface, at bottom of binder layer and geosynthetic reinforcement at middle of base layer, shows that there is a noticeable change in case steel reinforcement at middle of base layer. In this location the lateral strain ϵ_Y is decreased to $3.16E-05$ i.e. decreasing percent is 75.5% from without reinforcement case then arrived to $2.65E-04$ at bottom of base layer i.e. 26.6% decreasing percent from the lateral strain ϵ_Y in ordinary case. Figures also illustrate that there is a drastic change in the lateral strain ϵ_Y values when the steel reinforcement at bottom of base layer, lateral strain ϵ_Y in this location was $5.90E-05$ i.e. decreasing percent is 83.60% from its value in without reinforcement case. While in case of reinforcement with geosynthetic at same location lateral strain ϵ_Y was $3.15E-04$ i.e. decreasing percent is 12.55% from its value in without reinforcement case.

Figures (13) and (14) for freeway section show that there is a noticeable change when we add the steel reinforcement at middle of base layer, the lateral strain ϵ_Y is decreased to $4.96E-05$ i.e. 72.01% decreasing percent from without reinforcement case ($1.77E-04$) then arrived to $1.94E-04$ at bottom of base layer i.e. 33.30% decreasing percent from the strain in ordinary case. And illustrate that there is a drastic change in lateral strain ϵ_Y values when the steel reinforcement was at bottom of base layer. The lateral strain ϵ_Y arrived in this location to $5.39E-05$ i.e. decreasing percent is 81.50% from its value in without reinforcement case. While for case of reinforcement with geosynthetic the lateral strain ϵ_Y arrived in this location to $2.61E-04$ i.e. decreasing percent is 10.62% from its value in without reinforcement case. Figures show that there is no change in lateral strain ϵ_Y distribution in others cases and case without reinforcement.

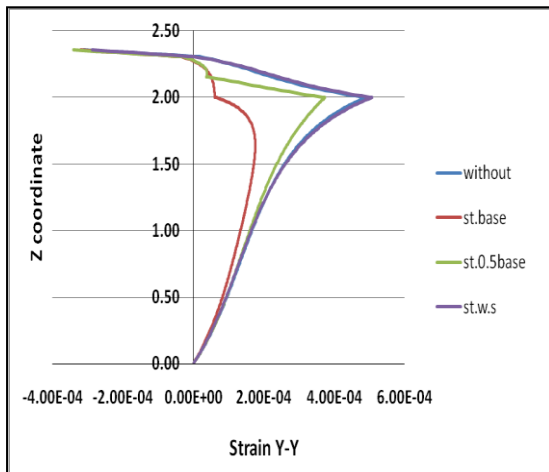


Fig. 9. Lateral strain ϵ_Y due to vertical pressure of wheel versus section depth for local road section with and without steel reinforcement

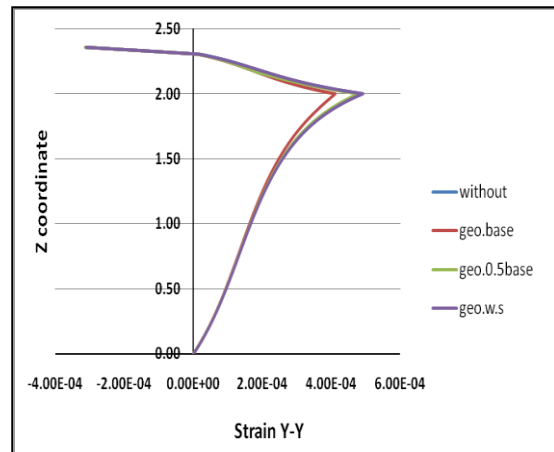


Fig. 10. Lateral strain ϵ_Y due to vertical pressure of wheel versus section depth for local road section with and without geosynthetics reinforcement

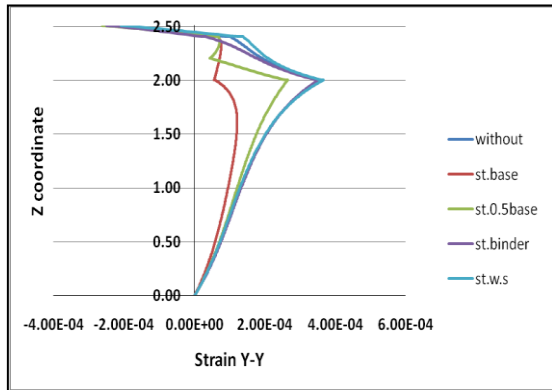


Fig. 11. Lateral strain ϵ_Y due to vertical pressure of wheel versus section depth for expressway section with and without steel reinforcement

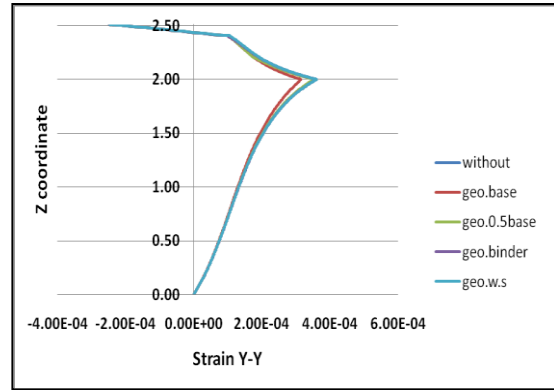


Fig. 12. Lateral strain ϵ_Y due to vertical pressure of wheel versus section depth for expressway section with and without geosynthetic reinforcement

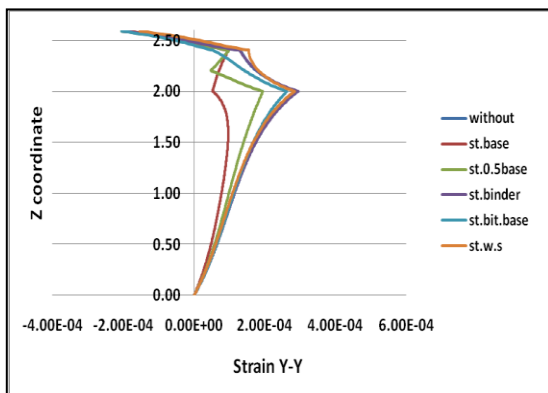


Fig. 13. Lateral strain ϵ_Y due to vertical pressure of wheel versus section depth for freeway section with and without steel reinforcement

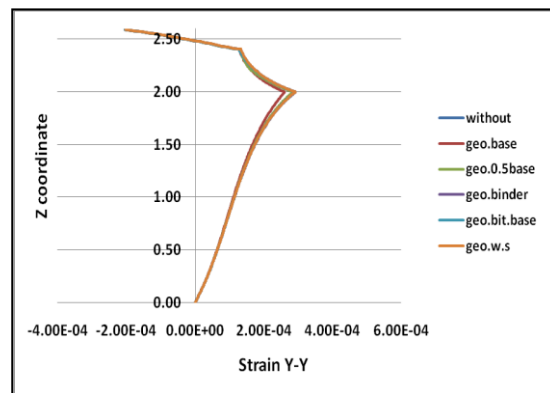


Fig. 14. Lateral strain ϵ_Y due to vertical pressure of wheel versus section depth for freeway section with and without geosynthetic reinforcement

4.2 Results of sections affected by vertical loads and friction force

4.2.1 Vertical stress

Figures (15) to (20) present the variation of vertical stress σ_Z at bottom of base layer in studied sections vertical pressure of wheel and horizontal force due to friction and illustrate the effect of adding reinforcement with different locations. Figures (15) and (16) for local road section show that the vertical stress σ_Z in without reinforcement case start increase from $-4.00E+04$ Pa under the center line of the wheel load to $-4.15E+04$ Pa at 0.17 m from center line of the wheel load and then decreases to decay at the end of section width. Figures also show that there is no change in cases reinforcement at bottom of wearing surface. Figures also show that there is a noticeable change after adding the steel reinforcement at middle of base layer the steel reinforcement at middle of base layer, the vertical stress σ_Z start increase from $-3.64E+04$ Pa i.e. decrease percent is 8.9% under the center line of the wheel load to $-3.88E+04$ Pa i.e. decrease percent is 12.29% at 0.17 m from center line of the wheel load and then decreases to decay at the end of section width, while for case of reinforcement with geosynthetic there is no change.

Figures illustrate that there is a drastic change in vertical stress σ_Z values when the steel reinforcement was added at bottom of base layer, The vertical stress σ_Z start increase from $-2.04E+04$ Pa i.e. decrease percent is 48.75% under the center line of the wheel load to $-2.14E+04$ Pa i.e. decrease percent is 48.47% at 0.17 m from center line of the wheel load and then decreases to decay at the end of section width, while in case of reinforcement with geosynthetic ,the vertical stress σ_Z start increase from $-2.56E+04$ Pa i.e. decrease percent is 35.91% under the center line of the wheel load to $-2.68E+04$ Pa i.e. decrease percent is 35.45% at 0.17 m from center line of the wheel load and then decreases to decay at the end of section width.

Figures (17) and (18) for expressway section show that the vertical stress σ_Z in without reinforcement case start increase from $-3.13E+04$ Pa under the center line of the wheel load to $-3.14E+04$ Pa at 0.17 m from center line of the wheel load and then decreases to decay at the end of section width. Figures also show that there is a noticeable change when we add the steel reinforcement at middle of base layer, the vertical stress σ_Z start increase from $-2.86E+04$ Pa i.e. decrease percent is 8.5% under the center line of the wheel load to -

2.88E+04 Pa i.e. decrease percent is 8.29% at 0.20 m from center line of the wheel load and then decreases to decay at the end of section width. Figures also illustrate that there is a drastic change in vertical stress σ_z values when the steel reinforcement was added at bottom of base layer, The vertical stress σ_z start from -1.62E+04 Pa i.e. decrease percent is 48.5% under the center line of the wheel load and still at same value to 0.17 m from center line of the wheel load and then decreases to decay at the end of section width, while in case of reinforcement with geosynthetic The vertical stress σ_z start from -2.00E+04 Pa i.e. decrease percent is 36% under the center line of the wheel load and still at same value to 0.17 m from center line of the wheel load and then decreases to decay at the end of section width. Figures show that there is no change in vertical stress σ_z distribution in others cases and the case without reinforcement.

Figures (19) and (20) for freeway section display that the vertical stress σ_z in without reinforcement case start from -2.67E+04 Pa under the center line of the wheel load and still at same value to 0.17 m from center line of the wheel load and then decreases to decay at the end of section width. Figures also show that there is no change in cases reinforcement at bottom of wearing surface and at bottom of binder layer. Figures also show that there is a noticeable change when we add the steel reinforcement at the end of bituminous base layer, the vertical stress σ_z start from -2.55E+04 Pa i.e. decrease percent is 4.31% under the center line of the wheel load and still at same value to 0.17 m from center line of the wheel load and then decreases to decay at the end of section width, while there is no change in geosynthetic reinforcement at same location. Figures also show that there is a noticeable change when we add the steel reinforcement at middle of base layer, the vertical stress σ_z start from -2.38E+04 Pa i.e. decrease percent is 10.77% under the center line of the wheel load and still at same value to 0.17 m from center line of the wheel load and then decreases to decay at end of section width. Figures also show that there is a drastic change in vertical stress σ_z values when the reinforcement was added at bottom of base layer. The vertical stress σ_z start from -1.39E+04 Pa i.e. decrease percent is 48% under the center line of the wheel load and still at same value to 0.17m from center line of the wheel load and then decreases to decay at end of section width, while in case of reinforcement with geosynthetic, the vertical stress σ_z start from -1.70E+04pa i.e. decrease percent is 35.9% under the center line of the wheel load and still at same value to 0.17 m from center line of the wheel load and then decreases to decay at end of section width.

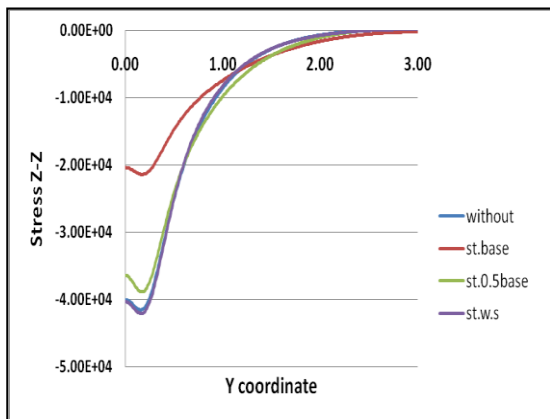


Fig. 15. Vertical stress σ_z due to vertical pressure of wheel and friction force at bottom of base layer for local road section with and without steel reinforcement

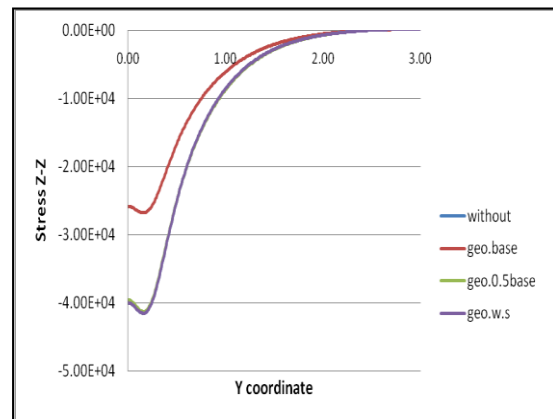


Fig. 16. Vertical stress σ_z due to vertical pressure of wheel and friction force at bottom of base layer for local road section with and without geosynthetics reinforcement

4.2.2 Lateral strain

Figures (21) to (26) present the variation of lateral strain under the center line of the wheel through the depth of the studied sections due to vertical pressure of wheel and horizontal friction force. Figures (21) and (22) for local road section exhibit that the lateral strain ϵ_y start increase from 2.22E-04 at surface to 3.45E-04 at bottom of wearing surface layer then decrease to 2.15E-04 at 160mm from surface layer then increase to 3.61E-04 at bottom of base layer and then decreases to decay. But for steel reinforcement at middle of base layer the lateral strain ϵ_y start increase from 1.73E-04 at surface to 2.81E-04 at 60mm from surface then decrease to 5.12E-05 at middle of base then increase to 2.08E-04 i.e. 42.35% of ordinary value at bottom of base layer then decreases to decay.

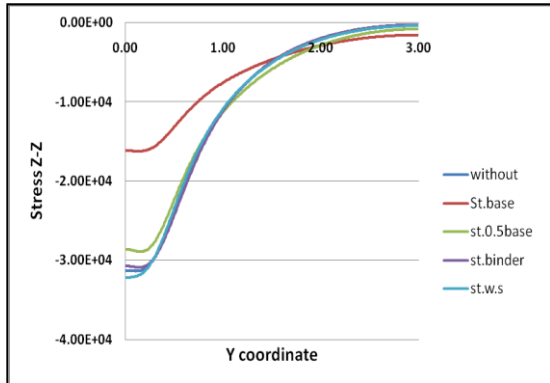


Fig. 17. Vertical stress σ_z due to vertical pressure of wheel and friction force at bottom of base layer for expressway section with and without steel reinforcement

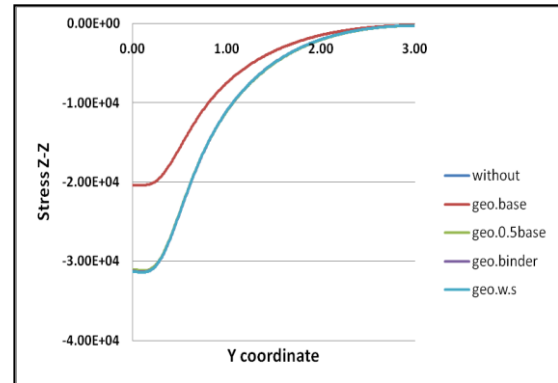


Fig. 18. Vertical stress σ_z due to vertical pressure of wheel and friction force at bottom of base layer for expressway section with and without geosynthetic reinforcement

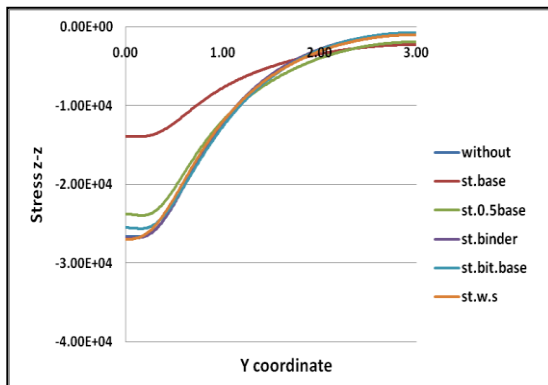


Fig. 19. Vertical stress σ_z due to vertical pressure of wheel and friction force at bottom of base layer for freeway section with and without steel reinforcement

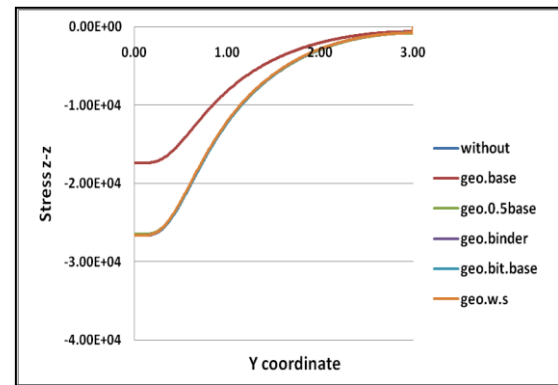


Fig. 20. Vertical stress σ_z due to vertical pressure of wheel and friction force at bottom of base layer for freeway section with and without geosynthetic reinforcement

Figures also show the lateral strain ϵ_y in geosynthetic reinforcement at bottom of base layer decreased by 10.8% from values in without reinforcement case. And for steel reinforcement the lateral strain ϵ_y start increase from $1.97E-04$ at surface to $2.90E-04$ at 60mm from surface then decrease $6.06E-05$ at bottom of base layer i.e. decreasing percent is 83.60% from its value in without reinforcement case and then decreases to decay.

Figures (23) and (24) for expressway section show that the horizontal lateral strain ϵ_y start increase from $1.84E-04$ at surface to $1.91E-04$ at 20mm from surface layer then decrease to $1.11E-04$ at 180mm from surface layer then increase to $2.32E-04$ at bottom of base layer then decreases to decay. Figures show in case steel reinforcement at bottom of wearing surface layer the lateral strain ϵ_y start increase from $9.85E-05$ at surface to $1.04E-04$ at 10mm from surface then decrease to $6.18E-05$ at 50mm from surface layer then increase to $2.79E-04$ at surface of sub grade and then decreases to decay. Figures also show in case of steel reinforcement at bottom of binder layer the lateral strain ϵ_y start increase from $1.41E-04$ at surface to $1.46E-04$ at 10mm from surface then decrease to $4.96E-05$ at 160mm from surface layer then increase to $2.40E-04$ i.e. 10% of original case at surface of sub grade and then decreases to decay. Figures also show in case of steel reinforcement at middle of base layer the lateral strain ϵ_y start increase from $1.66E-04$ at surface to $1.71E-04$ at 10mm from surface then decrease to $4.00E-05$ at 250mm from surface layer then increase to $1.66E-04$ i.e. 37.9% of ordinary value at surface of sub grade and then decreases to decay. Figures also illustrates that no change in the lateral strain ϵ_y values between adding the geosynthetic reinforcement at bottom of base layer and the case without reinforcement from surface to subgrade but the lateral strain ϵ_y at surface of subgrade decreased by 10.8% from the lateral strain ϵ_y in without reinforcement case. And for steel reinforcement the lateral strain ϵ_y start increase from $1.85E-04$ at surface to $1.89E-04$ at 10mm from surface then decrease to $4.44E-05$ at 290 mm from surface layer then increased to $5.11E-05$ i.e. 80.75% of ordinary value at bottom of base layer and then decreases to decay. Figures show that there is no change in lateral strain ϵ_y distribution in others cases and the case without reinforcement.

Figures (25) and (26) for freeway section clarify that the lateral strain ϵ_Y start increase from 1.48E-04 at surface to 1.55E-04 at 20mm from surface layer then decrease to 6.98E-05 at 190mm from surface layer then increase to 2.13E-04 at bottom of base layer and then decreases to decay. For steel reinforcement at bottom of wearing surface the lateral strain ϵ_Y start increase from 8.00E-05 at surface to 8.65E-05 at 10mm from surface then decrease to 4.63E-05 at 50mm from surface layer then increase to 2.27E-04 at bottom of base layer and then decreases to decay. In case of steel r at bottom of binder layer the lateral strain ϵ_Y start increase from 1.29E-04 at surface to 1.35E-04 at 10mm from surface then decrease to 4.96E-05 at 110mm from surface layer then increase to 2.10E-04 at bottom of base layer and then decreases to decay. Figures show in case steel reinforcement at bottom of bituminous base layer the lateral strain ϵ_Y start increase from 1.27E-04 at surface to 1.32E-04 at 20mm from surface then decrease to 4.14E-05 at 190mm from surface layer then increase to 1.79E-04 i.e. 16% of ordinary value at bottom of base layer and then decreases to decay.

Figures also present that no change in the lateral strain ϵ_Y values between adding the geosynthetic reinforcement at the middle of base layer and the case without reinforcement from surface to subgrade but the lateral strain ϵ_Y at surface of subgrade decreased by 10.8% from the lateral strain ϵ_Y in without reinforcement case, while for steel reinforcement at the same location the lateral strain ϵ_Y start increase from 1.44E-04 at surface to 1.48E-04 at 10mm from surface then decrease to 3.59E-05 at 250mm from surface layer then increase to 1.23E-04 i.e. 42.16% of ordinary value at bottom of base layer and then decreases to decay. Figures also illustrate that no change in the lateral strain ϵ_Y values between adding the geosynthetic reinforcement at bottom of base layer and the case without reinforcement from surface to subgrade. But the lateral strain ϵ_Y at surface of subgrade decreased by 8% from the lateral strain ϵ_Y in without reinforcement case, while for steel reinforcement the lateral strain ϵ_Y start increase from 1.59E-04 at surface to 1.63E-04 at 10mm from surface then decrease to 4.44E-05 at 170 mm from surface layer then increased to 4.63E-05 i.e. 78.30% of ordinary value at bottom of base layer then decreases to decay. Figures show that there is no change in lateral strain ϵ_Y distribution in others cases and the case without reinforcement.

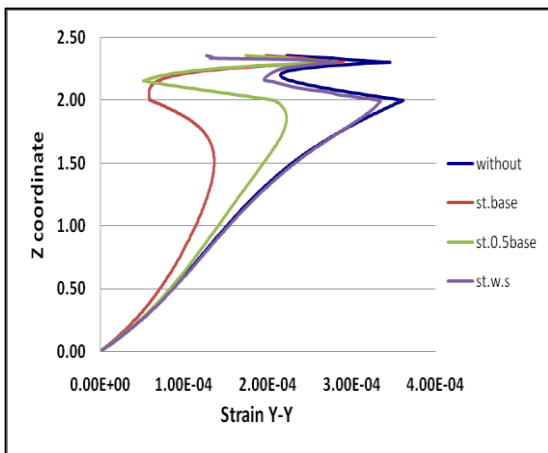


Fig. 21. Lateral strain ϵ_Y due to vertical pressure of wheel and friction force versus section depth for local road with and without steel reinforcement

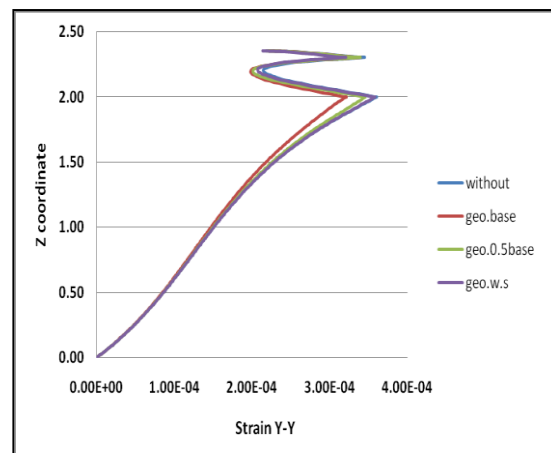


Fig. 22. Lateral strain ϵ_Y due to vertical pressure of wheel and friction force versus section depth for local road section with and without geosynthetic reinforcement

4.3 Comparison between the reinforced flexible pavements sections and rigid pavement section

4.3.1 Vertical stress

The variation of vertical stress σ_z at top of subgrade for studied paving sections with steel or geosynthetic reinforcement and selected rigid pavement section 20cm reinforced concrete slab with steel diameter is 8 mm and rested on 15cm sub base layer is shown in figures (27) and (28). From figure (27) it is clear that the values of vertical stress σ_z in section reinforced with steel mesh are lower than the values in section reinforced with geosynthetic. Figure (28) show that the value of vertical stress σ_z under the wheel in rigid pavement section is lower with 15.93% than value in local road section reinforced with steel, but it is greater with 15.64% than values in expressway section reinforced with steel and greater with 29.85% than the stress in freeway section reinforced with steel.

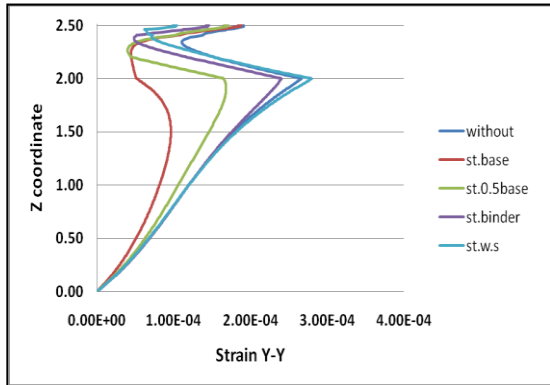


Fig. 23. Lateral strain ϵ_Y due to vertical pressure of wheel and friction force versus section depth for expressway section with and without steel reinforcement

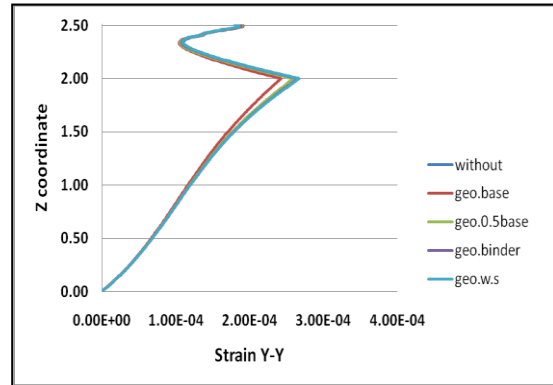


Fig. 24. Lateral strain ϵ_Y due to vertical pressure of wheel and friction force versus section depth for expressway section with and without geosynthetics reinforcement

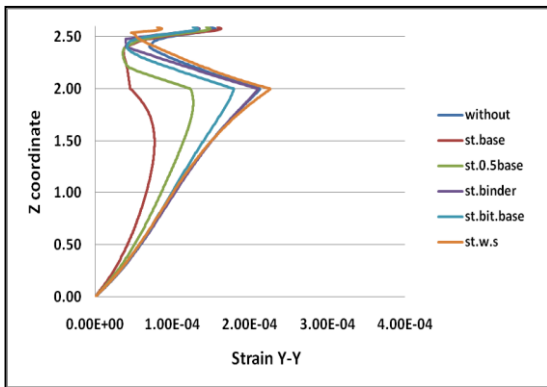


Fig. 25. Lateral strain ϵ_Y due to vertical pressure of wheel and friction force versus section depth for freeway section with and without steel reinforcement

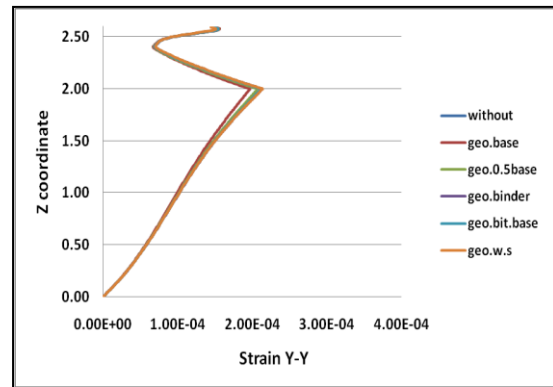


Fig. 26. Lateral strain ϵ_Y due to vertical pressure of wheel and friction force versus section depth for freeway section with and without geosynthetics reinforcement

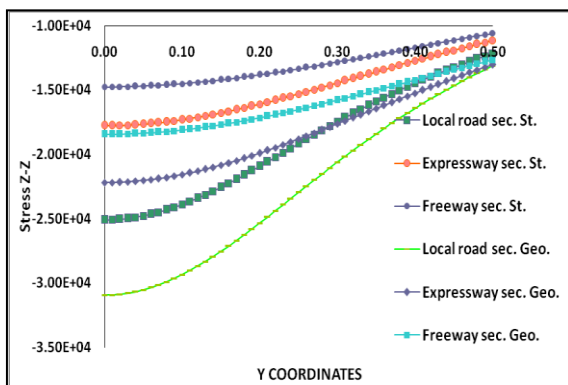


Fig. 27. Vertical stress σ_Z due to vertical pressure of wheel at bottom of base layer for investigated sections with steel reinforcement or geosynthetics reinforcement

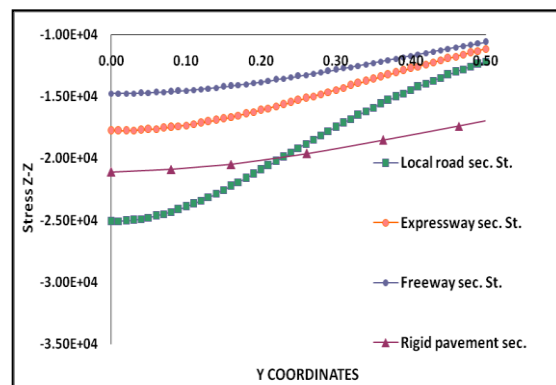


Fig. 28. Vertical stress σ_Z due to vertical pressure of wheel at bottom of base layer for investigated sections with steel reinforcement or rigid pavement

4.3.2 Lateral strain

Lateral strain ϵ_Y values under the centerline of the wheel load at top of subgrade for studied sections with steel or geosynthetic reinforcement and selected rigid pavement section (20cm reinforced concrete slab with steel diameter is 8 mm and rested on 15cm sub base layer) are shown in Table (5). From this table it is clear that the values of lateral strain ϵ_Y in steel reinforced sections are decreased than its values in geosynthetic reinforced sections. Table also shows that the values of lateral strain ϵ_Y in rigid pavement section are lower with 7% than value in local road section reinforced with steel but it is greater with 1.1% than values in expressway section reinforced with steel and greater with 12.50% than the stress in freeway section reinforced with steel.

Table 5. Lateral strain ϵ_y at top of subgrade due to vertical pressure of wheel for studied sections with steel reinforcement or geosynthetics reinforcement and rigid pavement section

Reinforcement Type	Section	Lateral Strain
Geosynthetics Reinforcement	Local Road	4.12E-04
	Expressway	3.15E-04
	Freeway	2.61E-04
Steel Reinforcement	Local Road	6.52E-05
	Expressway	5.90E-05
	Freeway	5.39E-05
Rigid Pavement Section		5.80E-05

V. CONCLUSION

Based on the previous analysis the following conclusions are given:

1. Bottom of base layer was found to be the most suitable location of reinforcing where the maximum reduction in vertical stress and lateral strain is occurred in all investigated sections.
2. Vertical stress σ_z under middle of wheel at bottom of base layer in steel wire grid reinforced paving sections subjected to vertical load due to wheel pressure only is decreased with about 48% from without reinforcement cases in the investigated three sections, while in geosynthetic reinforcement cases the decreasing percent is about 35% from without reinforcement cases.
3. In cases paving sections subjected to vertical load due to wheel pressure and horizontal friction force, the vertical stress σ_z under center line of wheel at bottom of base layer in steel wire grid reinforced cases is decreased with about 48.75% from without reinforcement cases in the investigated three sections, while in geosynthetic reinforcement cases the decreasing percent is about 36% from without reinforcement cases.
4. Lateral strain ϵ_y under the centerline of the wheel load at the bottom of base layer in steel wire grid reinforced paving sections subjected to vertical load due to wheel pressure only is decreased from without reinforcement sections, with 86.70% in local road section, 83.60% in expressway section and 81.50% in freeway section, while in geosynthetic reinforcement cases the decreasing percents are 16%, 12.55% and 10.62% respectively.
5. In cases paving sections subjected to vertical load due to wheel pressure and horizontal friction force, lateral strain ϵ_y under the centerline of the wheel load at the bottom of base layer in steel wire grid reinforced cases is decreased from without reinforcement sections with 83.60% in local road section, 80.75% in expressway section and 78.30% in freeway section, while in geosynthetic reinforcement cases the decreasing percents are 10.8% in sections local road section and expressway section while 8% for freeway section.
6. Lateral strain ϵ_y under the centerline of the wheel load at top of subgrade in selected rigid pavement section is lower with 7% than value in local road section reinforced with steel but it is greater with 1.1% than values in expressway section reinforced with steel and greater with 12.50% than the stress in freeway section reinforced with steel.
7. Vertical stress σ_z at top of subgrade in selected rigid pavement section is lower with 15.93% than value in local road section reinforced with steel, but it is greater with 15.64% than values in expressway section reinforced with steel and greater with 29.85% than the stress in freeway section reinforced with steel.
8. Investigators recommend in future work:
 - An economic study to assess the benefit of using proposed strengthening technique.
 - Enhance the analysis to include the environmental effects on the reinforced paving sections.
 - Investigate the effect of dynamic loading on the reinforced paving sections.

REFERENCES

- [1] Al-Qadi, I.L., Elseifi, M. and Leonard D., 2007. Development of an overlay design model for reflective cracking with and without steel reinforcing netting. AAPT Conference.
- [2] Choi, S.K., 2009. FLOWMEC – A 3-dimensional finite element code for the modelling of multiphysics problems.
- [3] Nods, M., 2000. Effectiveness of asphalt reinforcement with geogrids. Huesker Synthetic.
- [4] Vuong, B.T., 2005. Initial development of models to predict pavement wear under heavy vehicles. Austroads Project No: T+E.P.N.537. Austroads Report. ARRB Group Ltd.
- [5] Hadi MNS, Bodhinayake BC. Non linear finite element analysis of flexible pavements. Adv Eng Soft 2003; 34(3):657–62.
- [6] Bassam Saad, Hani Mitri and Hormoz Poorooshasb. 3D FE Analysis of Flexible Pavement with Geosynthetic Reinforcement. Journal of transportation engineering © ASCE / MAY 2006.

- [7] Vuong, B.T. and Choi, X., 2009. Modelling of responses of road pavements containing reinforced materials. Contract Report for RTA-NSW. ARRB Group Ltd. (Unpublished).
- [8] H. Akbulut, K. Aslatas. Finite element analysis of stress distribution on bituminous pavement and failure mechanism. *Materials and design* 26(2005)383-387.
- [9] ADINA 8.7.3 Manuals (2005) ADINA R&D, Inc. Watertown, MA, USA.
- [10] Egyptian Code for roads, part (4) Road construction materials and tests, Egypt 2008.
- [11] Specifications of General Authority for Roads and Bridges, Egypt 1990
- [12] Finite element modelling of flexible pavements on soft soil subgrades R.M. Mulungye, P.M.O. Owende, K. Mellon. *Materials and Design* 28 (2007) 739–756.